ONCOLOGY

The carcinogenic capacity of arsenic in normal epithelial breast cells and double-positive breast cancer cells

Alina-Andreea Zimta[1,2], Diana Cenariu[1], Adrian Bogdan Tigu[1], Cristian Moldovan[1], Ancuta Jurj[2], Laura Pop[2], Ioana Berindan-Neagoe[2]

1) MedFuture Research Center for Advanced Medicine, Iuliu Hatieganu University of Medicine and Pharmacy, Cluj-Napoca, Romania

2) Research Center for Functional Genomics, Biomedicine and Translational Medicine, Iuliu Hatieganu University of Medicine and Pharmacy, Cluj-Napoca, Romania

Abstract

Background and aims. The carcinogenic effect of arsenic is a subject of controversy in relation to breast cancer. In our current research, we aimed to simulate the effects of chronic low-level arsenic exposure on breast cells by intoxicating MCF-10A and MCF-7 cells with 1 µM Arsenic trioxide (As2O3) for 3 weeks (3w) and 6 weeks (6w), respectively.

Methods. We assessed the cellular responses to As2O3 through various assays, including confocal fluorescence microscopy, flow cytometry for cell cycle analysis, Transwell invasion assay, scratch assay, and colony assay. Additionally, we analyzed the mutation burden in all the exposed cells by using the next generation sequencing technology.

Results. Our findings indicate that As2O3 has a minor carcinogenic effect in normal cells, with no definitive evidence of malignant transformation observed after 6 weeks of exposure. In the case of breast cancer cells, As2O3 exhibits a dual effect, both inhibitory and stimulatory. It leads to reduced colony formation ability at 6 weeks, while enhancing the cells' ability for invasion. The mutations triggered by As2O3 exposure are distributed across genes with both tumor-suppressive and oncogenic functions. Five mutations are common to both cell lines, involving the following genes: *Kinase Insert Domain Receptor (KDR)* (c.798+54G>A), *Colony Stimulating Factor 1 Receptor (CSF1R)* (c.*37AC>C, c.*35C>TC), *SWI/SNF-Related Matrix-Associated Actin-Dependent Regulator of Chromatin Subfamily B Member 1 (SMARCB1)* (c.1119-41C>T), and *Fms-like Tyrosine Kinase 3 (FLT3)* (c.1310-3T>C). Additionally, *Human Epidermal Growth Factor Receptor 4 (ERBB4/HER4)* (c.421+58A>G) and *Human Epidermal Growth Factor Receptor 2 (HER2/ERBB2)* (c.2307+46A>G) mutations were exclusively found in MCF-10A cells exposed to As2O3. Furthermore, MCF-7 cells exhibited unique mutations in the *KIT Proto-Oncogene (KIT)* (c.1594G>A) and *TP53* (c.215C>G).

Conclusion. In summary, our study reveals that a 6-weeks exposure to arsenic has a limited carcinogenic effect in normal breast cells and a dual role in breast cancer cells.

Keywords: arsenic, breast cancer, heavy metals, carcinogenic, DNA mutations

DOI: 10.15386/mpr-2682

Manuscript received: 15.11.2023
Received in revised form: 03.12.2023
Accepted: 18.12.2023

Address for correspondence:
Alina-Andreea Zimta
zimta.alina.andreea@gmail.com

Background and aims

Breast cancer stands as the most prevalent cancer type among women globally, as revealed by 2020 GLOBOCAN data [1]. In recent times, there has been an increasing acknowledgment that, in most cases, breast cancer results from the interplay between genetic predisposition and environmental factors [2,3]. Arsenic, a metalloid, is nearly omnipresent in our environment. The primary route of human exposure to arsenic occurs through drinking water or consuming crops that have been contaminated, either through irrigation with arsenic-rich water or the application of insecticides and pesticides containing arsenic [4].

The human body is well adapted to metabolize and excrete this metalloid. Arsenic goes through a double methylation pathway in the liver through the activity of methyltransferase [4,5]. The toxicity of arsenic decreases with each methylation [4,5] and, more importantly, with the valency of methylated products. Monomethylarsonous acid (MMA(III)) and dimethylarsinous acid (DMA(III)) are markedly more toxic than inorganic arsenic, monomethylarsonic acid (MMA(V)) or dimethylarsinic acid (DMA (V)) [6,7].

The connection between arsenic and breast cancer is a topic of much debate. A 2020 review that summarized the epidemiological evidence related to breast cancer and arsenic concluded that there is still no final correlation being established. This uncertainty can be attributed to the failure to adequately account for contamination from various sources, the use of multiple types of biomarkers, and the lack of specificity in characterizing arsenic metabolites [8]. However, more recent studies from 2021 and 2022 have identified a positive link between breast cancer and arsenic. For example, an observational clinical trial examined arsenic levels in blood samples collected between 2010 and 2017. Then they tracked breast cancer incidence in these cases for an additional 4.5 years and found that women in the high percentile of arsenic exposure have a thirteen-fold increased risk of developing breast cancer [9]. Additionally, individuals with BReast CAncer gene 1(*BRCA1*) mutations who also have elevated levels of arsenic in their blood are at a higher risk of developing breast cancer compared to those with lower arsenic concentrations [10]. Furthermore, there is evidence connecting air pollution containing this metalloid to estrogen receptor-positive breast cancer in women in the United States [11]. These recent results suggest a potential link between arsenic exposure and breast cancer, though further research is needed to fully understand this relationship.

In the present study, we wanted to replicate the impact of arsenic (III) (specifically in the form of As_2O_3) on breast cancer within an experimental context. Our focus was on comparing its effects on a normal breast epithelial cell line (MCF-10A) with those on a double positive breast cancer cell line (MCF-7). We examined how these cells altered their responsiveness to arsenic, assessed changes in their intracellular morphology, investigated invasion and migration capabilities, and determined their potential for forming colonies. Additionally, we conducted an analysis of arsenic-induced DNA mutations by employing next-generation sequencing on the cells exposed to this element.

Methods

Cell culture and intoxication

The double positive breast cancer cell line, MCF-7 was maintained in Minimum Essential Medium (MEM) with added 10% fetal bovine serum (FBS), 1% glutamine (Glu) and 1% Penicillin-Streptomycin (Pen-Strep). For intoxication, 1 μM of As_2O_3 were added in the complete culture media for 3 weeks or 6 weeks. The normal epithelial cell line, MCF-10A (CRL-10317™) was cultured in 50% Mammary Epithelial Cell Growth Medium from Lonza (Gampel, Switzerland) and 50% High Glucose Dulbecco′s Modified Eagle′s Medium (DMEM) from Sigma Aldrich (ST. Louis, USA), with added 2% FBS, 1% Glu and 1% Pen-Strep. For intoxication of MCF-10A cells, 1 μM of As_2O_3 was added in the complete culture media for 3 weeks or 6 weeks. The cells were maintained in a humidified incubator at 5% CO_2 and 37 °C. The resulted intoxicated cell cultures were referred as: MCF-10A_As_2O_3_3w, MCF-10A_As_2O_3_6w, MCF-7_As_2O_3_3w and MCF-7_As_2O_3_6w.

Fluorescence confocal microscopy imaging

The cultured cells were seeded on a chamber slide for 24 h. First the working solution of MitoTracker from Thermo Fisher Scientific (Waltham, MS, USA) was added on the cultured cells in a 1/1 ratio. After 1h of incubation at 37 °C, the MitoTracker containing media was washed with PBS solution. The cells were fixed with 4% paraformaldehyde (PFA) for 10 minutes and permeabilized with 0.5% Triton X for 5 minutes. The cells were washed again, and Phalloidin-FITC from Cytoskeleton (Denver, CO, USA) was pipetted on top of the cells. The slides were incubated at room temperature (RT) for 30 minutes. Then the slides were washed with PBS and 100 nM of DAPI solution from Thermo Fisher Scientific (Waltham, MS, USA) was added. The images of the cells were taken with the Olympus FV1200 inverted confocal microscope (Tokyo, Japan), by using the line sequential mode. The Image J v.2.0 (https://imagej.nih.gov/ij) software was used for calibration, based on the provided metadata. The protocol for triple staining was described for the first time in [12].

Cell cycle evaluation through flow cytometry

The analysis of cell cycle progression affected by As_2O_3 exposure was done in the case of both long-term as well as short-term exposure. The MCF-10A_Ctr and MCF-7_Ctr were used as controls for calibration. For the long-term evaluation the MCF-10A_As_2O_3_3w, MCF-10A_As_2O_3_6w, MCF-7_As_2O_3_3w and MCF-7_As_2O_3_6w were tested. For short-term exposure evaluation, MCF-

10A cells (both controls and long-term intoxicated) were exposed to 2.5 µM of As_2O_3 for 24h, while the MCF-7 cell (all experimental settings) were exposed to 5 µM of As_2O_3. The difference in tested concentrations was because the MCF-10A cell lost viability when exposed to 5 µM of As_2O_3. The cells were recovered from culture and fixed with 1 mL of 70% ethanol solution. After 45 minutes of incubation at 4 °C, the cells were washed with PBS. The samples were then incubated at RT for additional 15 minutes with 500 µL of RNase buffer from Thermo Fisher Scientific (Waltham, MS, USA). For DNA staining, a propidium iodine (PI) solution of 2 mg/mL was added. After 30 minutes, the samples were pelleted and resuspended in 500 µL flow cytometry wash solution. Reading was done on the BD FACS Canto II Flow cytometer (San Jose, CA, USA).

Wound Healing Assay

The Culture-Insert 2 Well on µ-Plate 24 Well Black 14 mm from Ibidi GmbH (Gräfelfing, Germany) was utilized for scratch assay. Each half of the insert contained $1x10^4$ cells. The plates containing inserts were left to incubate at 37 °C, in the cell culture incubator for 24h. After this, the inserts were removed, and the cells were left to migrate. Pictures of the gap area were taken at different time intervals with the Olympus BX43 microscope (Tokyo, Japan) at the 10x magnification. The pictures were processed in the ImageJ software (National Institutes of Health, Bethesda, MD, USA) with the MiToBo plug in.

Transwell migration assay

The Transwell® inserts from Corning® (New York, United States) were coated with a 10% extracellular matrix (ECM) solution, named Geltrex from Thermo Fisher Scientific (Waltham, MA, USA). On top of the insert, 50µL of serum-free media with 2.5 x 10^4 cells was pipetted. On the bottom of the well, 100 µL FBS containing media was added. The plates were left in the incubator at 37 °C for 24h. For cell fixation a 4% PFA solution was used. The cells were then stained with 0.1% crystal violet solution for 5 minutes. The staining solution was washed, and pictures were taken with Olympus BX43 microscope (Tokyo, Japan) at the 10x magnification. Image processing and measurement were performed in the Image J program.

Colony assay

In the case of colony assay, 6-well plates were used. Initially, 500 cells/well were suspended in 2 mL of complete media and plated. The colonies were left to form and grow for 3 weeks in the cell culture incubator, set to the same conditions as in the case of general culture. The media was renewed every 2-3 days. After colony formation was observed, the media was removed from the wells and the colonies were fixed through 1h incubation at RT with 80% methanol solution. Staining was done with 0.5% crystal violet solution left to incubate for 2 minutes at RT. Pictures were taken with a digital camera and processed in Image J.

DNA extraction

For the DNA extraction, the commercially available kit Purelink genomic DNA isolation from Invitrogen (Massachusetts, USA) was used. More precisely, on top of 200 µL of cellular pellet, 20 µL of RNase and 20 µL of Proteinase was added. After 2 minutes of incubation at RT, the lysis buffer was added, followed by an incubation at 55 °C for 10 minutes. For DNA precipitation, 200 µL of pure ethanol were used. The DNA was separated with the help of columns provided by the kit. The columns containing the DNA were washed 2 times with the wash buffer. The DNA was diluted in 25 µL of ultrapure water and checked for purity and concentration at NanoDrop-1000 spectrophotometer from Thermo Scientific (Waltham, MS, USA).

DNA hotspot sequencing

20 ng of DNA were used for sequencing using the Ion AmpliSeq Cancer Hotspot Panel v2 (ThermoFischer Scientific) and the Ion AmpliSeq Library 2.0 kit (Thermofisher Scientific). The Ion AmpliSeq Cancer Hotspot Panel v2 consists of primers for hotspot evaluation in the following genes: Abelson Tyrosine-Protein Kinase 1 (*ABL1), RAC-Alpha Serine/Threonine-Protein Kinase (AKT1), Anaplastic Lymphoma Receptor Tyrosine Kinase (ALK), Adenomatous Polyposis Coli Protein (APC), Ataxia Telangiectasia Mutated (ATM), Serine/Threonine-Protein Kinase B-Raf (BRAF), Cadherin 1 (CDH1), Cyclin Dependent Kinase Inhibitor 2A (CDK2A), Colony Stimulating Factor 1 Receptor (CSF1R), Catenin Beta 1 (CTNNB1), Epidermal Growth Factor Receptor (EGFR), Erb-B2 Receptor Tyrosine Kinase 2 (ERBB2), Erb-B2 Receptor Tyrosine Kinase 4 (ERBB4), Enhancer Of Zeste 2 Polycomb Repressive Complex 2 Subunit (EZH2), F-Box And WD Repeat Domain Containing 7 (FBXW7), Fibroblast Growth Factor Receptor 1 (FGFR1), Fibroblast Growth Factor Receptor 2 (FGFR2), Fibroblast Growth Factor Receptor 3 (FGFR3), Fms Related Receptor Tyrosine Kinase 3 (FLT3), G Protein Subunit Alpha 11 (GNA11), G Protein Subunit Alpha Q (GNAQ), Guanine Nucleotide Binding Protein (G Protein), Alpha Stimulating Activity Polypeptide 1 (GNAS), Hepatocyte Nuclear Factor 1-Alpha (HNF1A), Isocitrate Dehydrogenase (NADP(+)) 1 (IDH1), Isocitrate Dehydrogenase (NADP(+)) 2 (IDH2), Janus Kinase 2 (JAK2), Janus Kinase 3 (JAK3),* Kinase Insert Domain Receptor *(KDR), KIT Proto-Oncogene, Receptor Tyrosine Kinase (KIT), Kirsten Rat Sarcoma Viral Oncogene Homolog (KRAS), Tyrosine-Protein Kinase Met (MET), MutL Homolog 1 (MLH1), Myeloproliferative Leukemia Protein (MPL), Neurogenic Locus Notch Homolog Protein 1 (NOTCH1), Nucleophosmin 1 (NPM1), Neuroblastoma RAS Viral Oncogene Homolog (NRAS), Platelet-Derived Growth Factor Receptor, Alpha Polypeptide (PDGFRA), Phosphatidylinositol-4,5-Bisphosphate 3-Kinase Catalytic Subunit Alpha (PIK3CA), Phosphatase And Tensin*

Homolog (PTEN), Protein Tyrosine Phosphatase Non-Receptor Type 11 (PTPN11), Retinoblastoma-Associated Protein (RB1), Rearranged During Transfection Protein (RET), Mothers Against Decapentaplegic Homolog 4 (SMAD4), SWI/SNF Related, Matrix Associated, Actin Dependent Regulator Of Chromatin, Subfamily B, Member 1 (SMARB1), Smoothened, Frizzled Class Receptor (SMO), Serine/Threonine Kinase 11 (STK11), Tumor Protein P53 (TP53), VHL. The sequencing libraries and the actual sequencing process were conducted according to the protocol described in our previous paper [13]. The data obtained after sequencing were analyzed using the Torrent Suit 5.6 and Ion Reporter 5.6 software for data trimming, alignment, and variant calling. The obtained variants were filtered using the following conditions: p value ≤ 0.05, coverage ≥500.

Statistical analysis

The statistical analysis was adapted to the type of raw data obtained from each laboratory test. Transwell and colony assay results were evaluated with ANOVA test. The scratch assay analysis was based on the Mixed-effect model. All the statistical tests and graphs (except flow cytometry) were built in GraphPad Software v.8. (San Diego, USA). The graphs for flow cytometry were made in Microsoft Office Excel. A p value <0.05 was considered statistically significant.

Results

Fluorescence confocal microscopy imaging results

Six weeks after being exposed to 1 μM As_2O_3, MCF-10A cells exhibited a significantly higher cell density compared to the control group, with limited signs of cellular stress, as evidenced by the presence of nuclei with a donut-like shape (orange arrow in Figure 1). On the other hand, the MCF-7 cells exposed for 6 weeks to 1μM of As_2O_3 showed more pronounced signs of stress, than in the case of MCF-10A_ As_2O_3_6w. There was a noticeable increase in the size of the cells. The cells appear to be multinucleated (as indicated by the red arrow in Figure 1). The cellular density was similar in MCF-7_Ctr and MCF-7_As_2O_3_6w. Remarkably, the MitoTracker images did not reveal any substantial changes between the samples.

Flow cytometry results for cell cycle

The outcomes of cell cycle analysis conducted on MCF-10A cells revealed that a three-week exposure to low concentrations of As_2O_3 did not have a noteworthy impact on the progression of the cell cycle. However, with an extended exposure period of six weeks, a distinct increase in the number of cells entering the G2/M phase was observed when compared to the control group (see Figure 2).

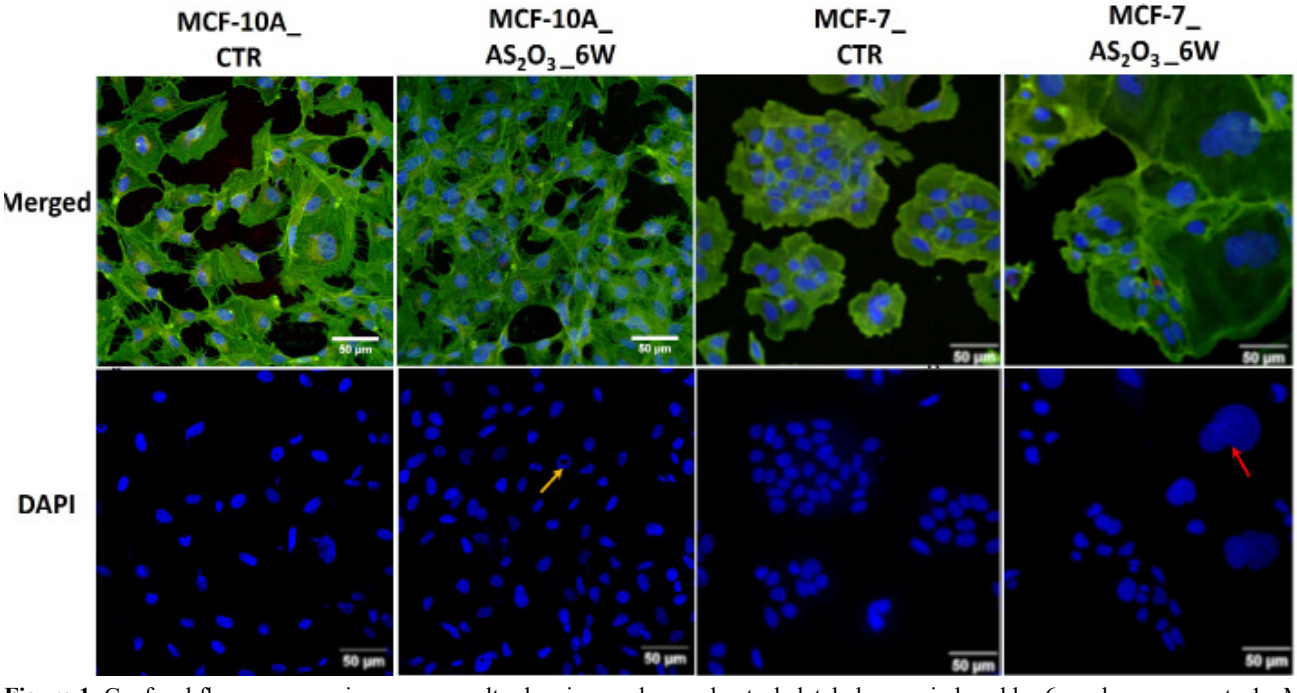

Figure 1. Confocal fluorescence microscopy results showing nuclear and cytoskeletal changes induced by 6 weeks exposure to 1 μM of As_2O_3 in MCF-10A and in MCF-7 cells. The upper panel contains the "merged" images, meaning a superposition of images obtained for Phalloidin-FITC (green) marking actin filaments of the cytoskeleton, MitoTracker (red) marking the mitochondria and DAPI (blue) marking the nuclei. The orange arrow stands for donut shaped nuclei. The red arrow shows multinucleated formations. The used magnification was 20x.

Specifically, in MCF-10A_CTR, 28% of cells were in the G2/M phase, whereas in MCF-10A_As_2O_3_6w, this percentage rose to 43%. Interestingly, there was no significant variance in cell cycle progression for MCF-7_As_2O_3_3w and MCF-7_As_2O_3_6w compared to the control group (Figure 2).

To investigate the effects of As_2O_3 on cell cycle progression under short-term exposure conditions, both MCF-10A and MCF-7 were exposed to increased doses of As_2O_3 for 24 hours (2.5 µM for MCF-10A and 5 µM for MCF-7) and subsequently analyzed using flow cytometry. MCF-10A_CTR and MCF-10A_As_2O_3_3w cells exhibited a distinct shift towards the G2/M phase, with 48% of cells found in G2/M phase in MCF-10A_Ctr + As_2O_3 (24h) and 43% in MCF-10A_ As_2O_3_3w + As_2O_3 (24h). The population of G2/M cells in MCF-10A_As_2O_3_6w + As_2O_3 (24h) remained similar to that of the MCF-10A_ As_2O_3_6w.

High-dose short-term treatment with As_2O_3 also stimulated the progression to G1 phase and G2 phase in MCF-7_CTR and MCF-7_ As_2O_3_3w, while lowering the number of cells found in G0. There were 43% G1 cells in MCF-7_CTR versus 63% in MCF-7_Ctr + As_2O_3 (24h) and 38% in MCF-7_ As_2O_3_3w versus 57% in MCF-7_ As_2O_3_3w + As_2O_3 (24h).

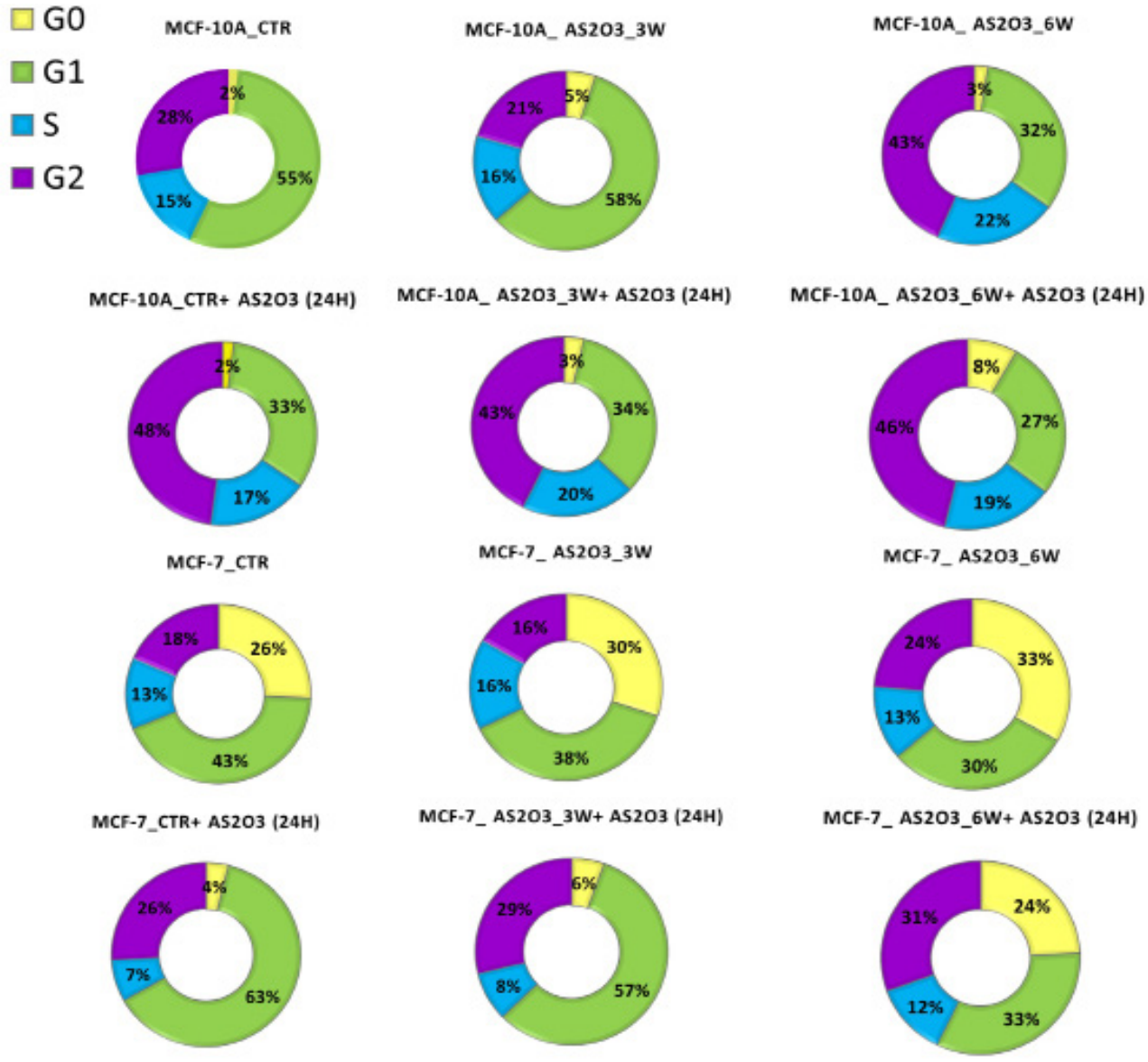

Figure 2. Doughnut charts based on the results from flow cytometry for cell cycle progression after long-term (3 weeks and 6 weeks) versus short-term (24h) exposure to As_2O_3. The long-term exposure was with 1 µM for MCF-10A and for MCF-7 cells. The short-term exposure was with 2.5 µM for MCF-10A and 5 µM for MCF-7. In the case of controls (CTR) there was no intoxication of As_2O_3. Each cell cycle phase is present in a different color: yellow-G0, green-G1, blue-S and violet-G2/M.

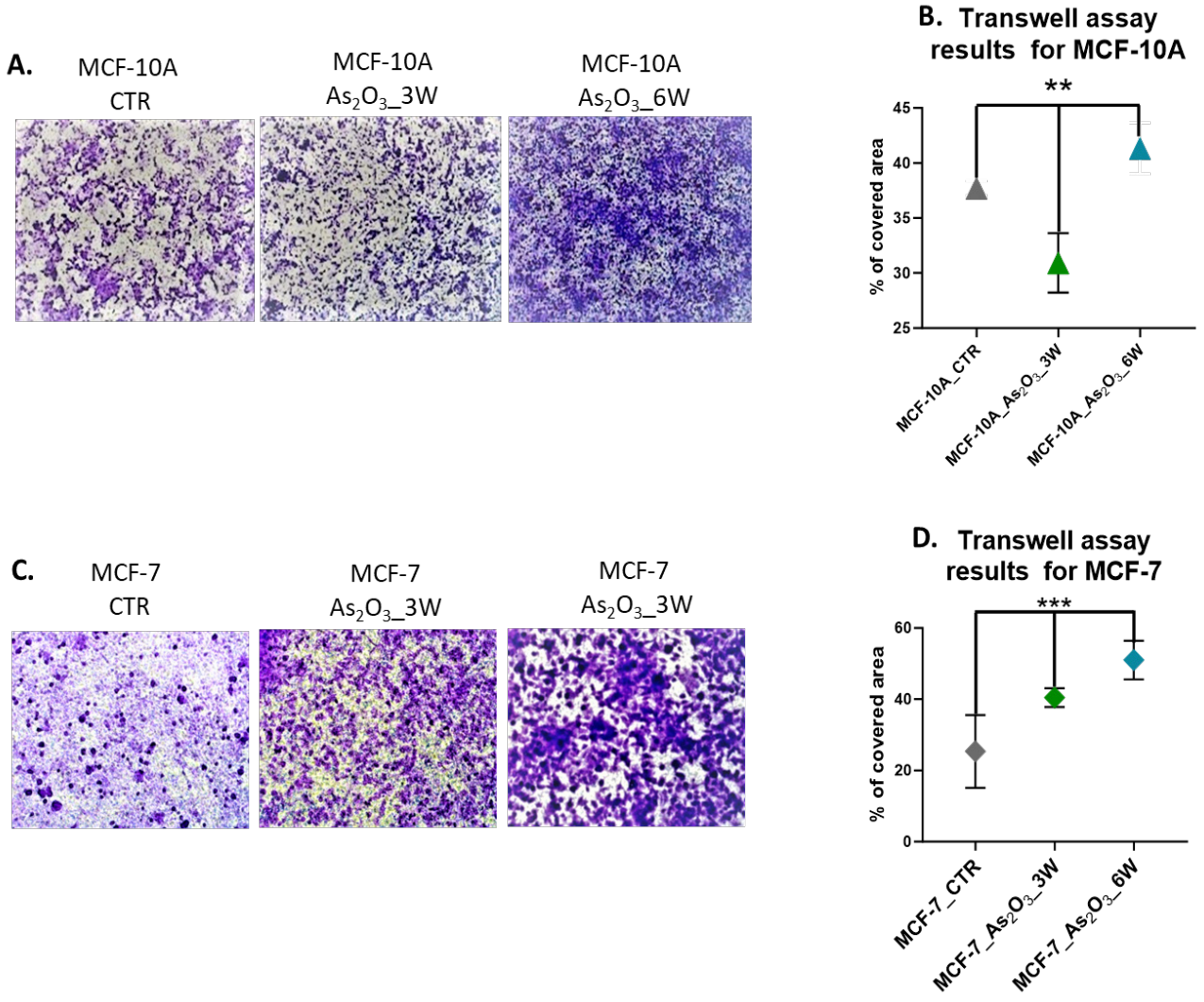

Figure 3. Transwell assay results **A.** Set of images containing examples of the analyzed field for each experimental condition, for MCF-10A cells. Images were taken at 4x magnification. **B.** Transwell assay results of image processing in Image J for MCF-10A cells in which % of covered area was analyzed. The box plot was done in GraphPad. **= p value ≤0.01. **C.** Transwell assay images containing examples of the analyzed fields for each experimental condition, in the case of MCF-7 cells. Images were taken at 4x magnification. **D.** Transwell assay results of imaging process in Image J for MCF-7 cells in which % of covered area was analyzed. The box plot was done in GraphPad. ***= p value ≤0.001.

There were 18% G2/M cells in MCF-7_CTR versus 26% in MCF-7_Ctr + As_2O_3 (24h) and 16% in MCF-7_ As_2O_3_3w versus 29% in MCF-7_ As_2O_3_3w + As_2O_3 (24h). In the case of cells intoxicated for 6 weeks there was no significant difference (Figure 2).

Transwell assay results

MCF-10A_As_2O_3_3w displayed a reduced invasive capacity when compared to MCF-10A_CTR. However, in the case of MCF-10A_As_2O_3_6w (as shown in Figure 3A and Figure 3B), a higher number of cells invaded the Transwell extracellular matrix compared to the control group (as indicated by a one-way ANOVA, p-value =0.0025). The mean (± standard deviation) of covered area had the following values: 37.71% (±0.65) for MCF-10A_CTR, 30.93% (±2.69) for MCF-10_As_2O_3_3w and 41.33% (±2.32) for MCF-10A_As_2O_3_6w.

Conversely, both MCF-7_As_2O_3_3w and MCF-7_As_2O_3_6w exhibited a higher number of cells invading the extracellular membrane in comparison to MCF-7_CTR (as depicted in Figure 3C and Figure 3D), with a one-way ANOVA yielding a p-value of 0.0007. The mean (± standard deviation) of covered area had the following values: 25.37% (±10.23) for MCF-7_CTR, 40.46% (±2.63) for MCF-7_ As_2O_3_3w and 51% (±5.40) for MCF-7_As_2O_3_6w.

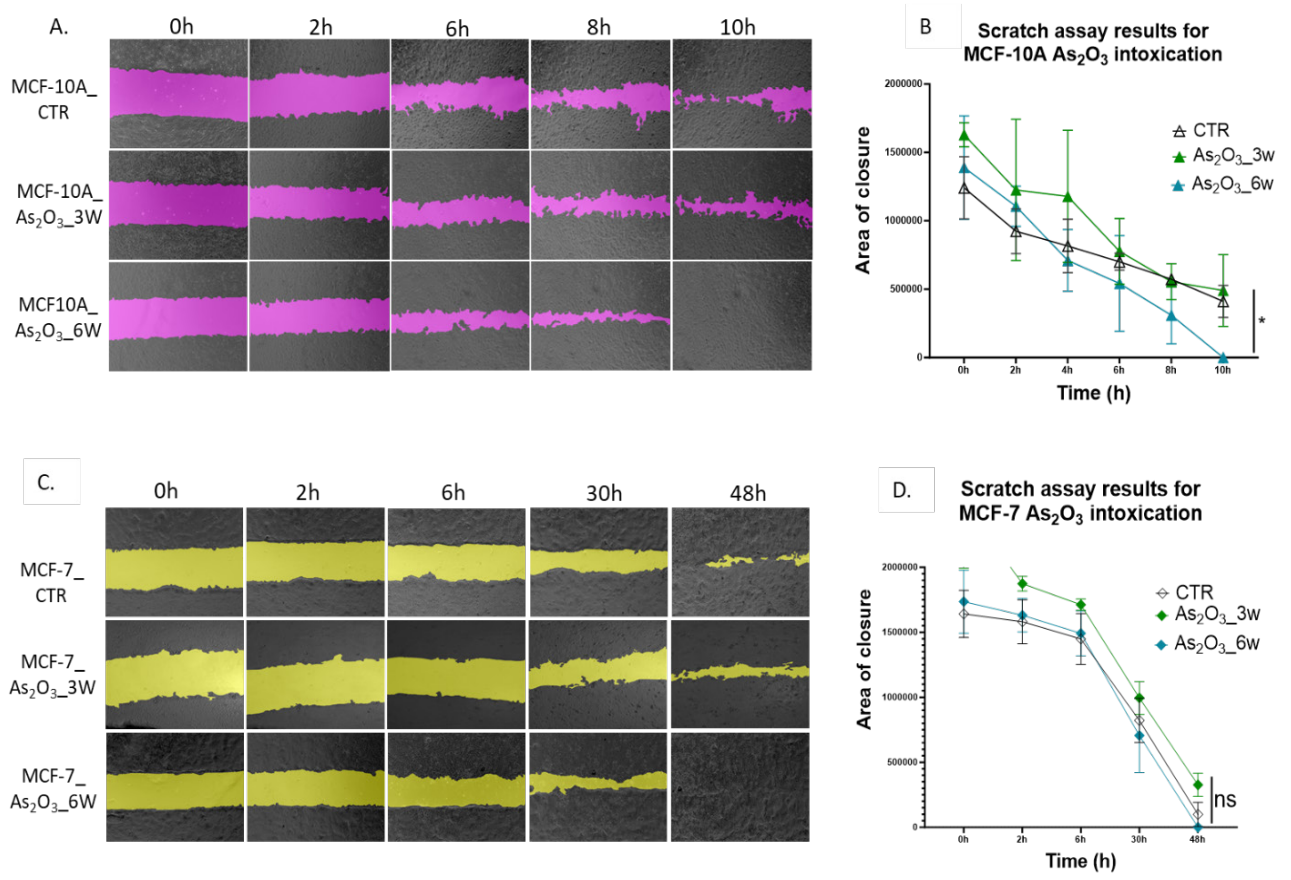

Figure 4. Scratch assay results: **A.** Scratch assay images for MCF-10A, processed in Image J (gap area marked on violet). Pictures were taken with an inverted microscope at 10x magnification, at different timepoints: 0h, 2h, 6h, 8h and 10h. **B.** Connecting lines of median symbols for gap area measurement for MCF-10A, as generated by GraphPad software. *= p value ≤0.05. **C.** Scratch assay images for MCF-7, processed in Image J (gap area marked on yellow). Pictures were taken with an inverted microscope at 10x magnification, at different timepoints: 0h, 2h, 6h, 30h and 48h. **D.** Connecting lines of median symbols for gap area measurement for MCF-7, as generated by GraphPad software. ns= p values was not statistically significant (≥ 0.05).

Scratch assay results

A statistically significant variance in gap closure was observed between the experimental conditions in the MCF-10A cell line (Mixed-effects model with REML, p value = 0.0271). Notably, MCF-10A_As_2O_3_3w cells exhibited a gap closure rate like that of the control group (as depicted in Figures 4A and 4B). However, the migration speed of MCF-10A_As_2O_3_6w cells surpassed that of both the control group and the cells exposed to As_2O_3 for 3 weeks (as depicted in Figure 4A and Figure 4B). Conversely, in the case of MCF-7 cells, the prolonged exposure to As_2O_3 had a relatively minor impact on the cells' migratory abilities that was not statistically significant (Mixed-effects model with REML, p value = 0.5064, as illustrated in Figure 4C and Figure 4D).

Colony assay results

The colony assay results reveal a gradual, time-dependent increase in the number of colonies in the case of MCF-10A cells (as depicted in Figure 5A and Figure 5B). While these results are statistically significant (confirmed through one-way ANOVA with a p-value of 0.0142), there isn't a substantial difference in the actual count of colonies, with MCF-10A_As_2O_3_6w having a maximum count of 5 colonies. These colonies were also relatively small and somewhat challenging to observe. The calculated means for colony numbers (± standard deviation) were as follows: 0.66 (±1.15) for MCF-10A_CTR, 2.33 (±0.57) for MCF-10A_As_2O_3_3w, and 4 (±1) for MCF-10A_As_2O_3_6w.

In the case of MCF-7 cells, three weeks of As_2O_3 exposure stimulated colony formation, while six weeks of exposure resulted in a decreased self-renewal capacity (as seen in Figure 5C and Figure 5D) (verified through one-way ANOVA with a p-value of 0.0216). The number of MCF-7_As_2O_3_3w colonies represented 122.61% of the control, while MCF-7_As_2O_3_6w exhibited several colonies that represented only 34.27% of the control group.

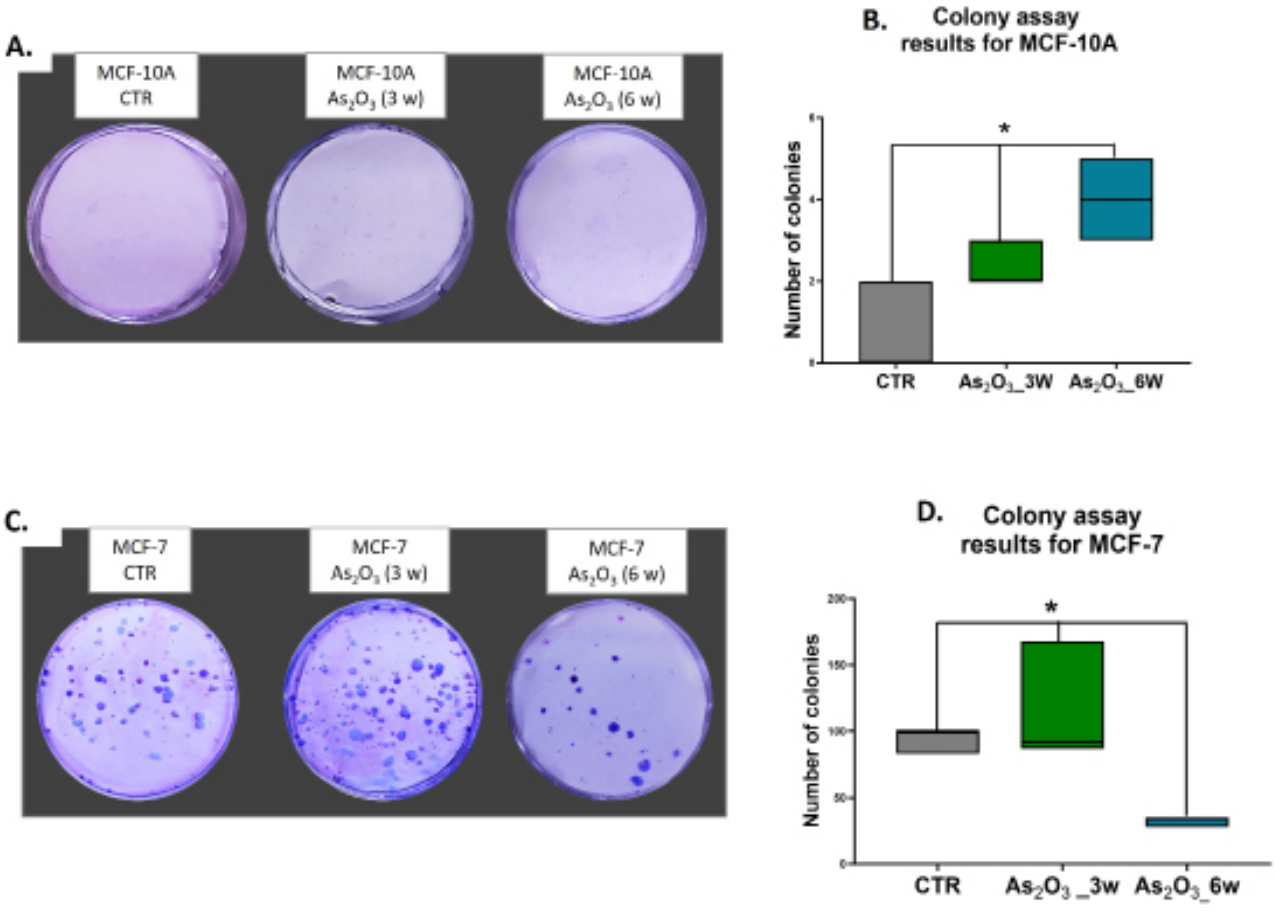

Figure 5. Colony assay results **A.** Picture of colonies one well/experimental condition, taken with digital camera for MCF-10A. **B.** Floating bar with median generated in Graph Pad based on image processing results from Image J for MCF-10A cell line. **C**. Picture of colonies one well/experimental condition, taken with digital camera for MCF-7. **D.** Floating bar with median generated in Graph Pad based on image processing results from Image J for MCF-7 cell line.

The means of colony numbers (± standard deviation) were as follows: 94.33 (±9.86) for MCF-7_CTR, 115.7 (±45.39) for MCF-7_As_2O_3_3w, and 32.33 (±3.78) for MCF-7_As_2O_3_6w.

The next generation sequencing results

As_2O_3 induces several mutations that were specific for the long-term exposed cells, MCF-10A_ As_2O_3_3w, MCF-10A_ As_2O_3_6w, MCF-7_ As_2O_3_3w and MCF-7_ As_2O_3_6w. These mutations were not detected in the controls. In both cell lines, in the exposed cells, three mutations exhibited a frequency exceeding 93%. These mutations were: *KDR* c.798+54G>A, *CSF1R* c.*37AC>C and *CSFR1* c.*35C>TC. Another mutation, *SMARCB1* c.1119-41C>T, displayed a variant frequency ranging from 48.55% to 52.3% and it was present in all intoxicated cells (as detailed in Table I).

FL3 c.1310-3T>C variant was absent in MCF-10A_As_2O_3_3w, but it displayed a frequency of 3.6% in MCF-10A_As_2O_3_6w. In MCF-7, this mutation was detected with a frequency of 50.45% in MCF-7_As_2O_3_3w and 47.97% in MCF-7_As_2O_3_6w (as described in Table I).

ERBB4 c.421+58A>G and *ERBB2* c.2307+46A>G were exclusively found in normal breast epithelial cells exposed to As_2O_3. For the mutated form of *ERBB4*, the frequency was 99.85% in MCF-10A_As_2O_3_3w and 100% in MCF-10A_As_2O_3_6w. *ERBB2* c.2307+46A>G appeared at a frequency of 47.65% at 3 weeks post-As_2O_3 intoxication and 48.95% at 6 weeks post-intoxication (as indicated in Table I).

Two other genes specifically displayed mutations in MCF-7 cells exposed to As_2O_3. These mutations were *KIT* c.1594G>A and *TP53* c.215C>G. The mutated form of *KIT* exhibited a frequency ranging between 49.67% at 6 weeks post-intoxication and 53.25% at 3 weeks post-intoxication. The mutated form of *TP53* (c215C>G) displayed a very high frequency in MCF-7 cells, exceeding 97% in the post-As_2O_3 exposure settings (as outlined in Table I).

Table I. The gene mutations driven by As_2O_3 long term exposure (3 weeks and 6 weeks) in MCF-10A and MCF-7 cells. The mutations were found through next generation sequencing panel of cancer-related genes, named Ion AmpliSeq Cancer Hotspot Panel v2. Abbreviations: w=weeks, I=intron, E=exon.

Sample	Gene	Coding	Transcript ID	% Frequency
MCF-10A_As_2O_3_3w	KDR	c.798+54G>A	NM_002253.3	98.52
MCF-10A_As_2O_3_6w				93.83
MCF-7_As_2O_3_3w				99.77
MCF-7_ As_2O_3_6w				98.55
MCF-10A_As_2O_3_3w	CSF1R	c.*37AC>C	NM_005211.3	99.09
MCF-10A_ As_2O_3_6w				100
MCF-7_As_2O_3_3w				99.52
MCF-7_ As_2O_3_6w				100
MCF-10A_As_2O_3_3w	CSF1R	c.*35C>TC	NM_005211.3	98.75
MCF-10A_ As_2O_3_6w				99.85
MCF-7_As_2O_3_3w				98.88
MCF-7_ As_2O_3_6w				99.39
MCF-10A_As_2O_3_3w	SMARCB1	c.1119-41C>T	NM_003073.5	52.3
MCF-10A_ As_2O_3_6w				49.05
MCF-7_As_2O_3_3w				51.11
MCF-7_ As_2O_3_6w				48.55
MCF-10A_As_2O_3_3w	FLT3	c.1310-3T>C	NM_004119.2	0
MCF-10A_ As_2O_3_6w				3.6
MCF-7_As_2O_3_3w				50.45
MCF-7_ As_2O_3_6w				47.97
MCF-10A_As_2O_3_3w	ERBB2	c.2307+46A>G	NM_004448.3	47.65
MCF-10A_ As_2O_3_6w				48.95
MCF-10A_As_2O_3_3w	ERBB4	c.421+58A>G	NM_005235.3	99.85
MCF-10A_ As_2O_3_6w				100
MCF-7_As_2O_3_3w	KIT	c.1594G>A	NM_000222.2	53.25
MCF-7_ As_2O_3_6w				49.67
MCF-7_As_2O_3_3w	TP53	c.215C>G	NM_000546.5	97.91
MCF-7_ As_2O_3_6w				97.38

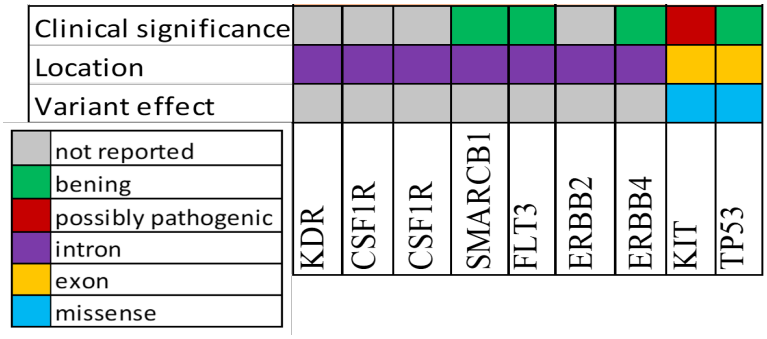

Figure 6. The characteristics of mutations detected in the exposed cells in the following genes: KDR, CSF1R, SMARCB1, FLT, ERBB2, ERBB4, KIT and TP53.

The mutations appearing in *KDR* c.798+54G>A, *CSF1R* c.*37AC>C, *CSF1R* c.*35C>TC, and *ERBB2* c.2307+46A>G have an unknown clinical significance, while *SMARCB1* c.1119-41C>T, *FLT3* c.1310-3T>C, *ERBB4* c.421+58A>G and *P53* c.215C>G have benign clinical significance. Only the mutation from *KIT* c.1594G>A has a potential pathogenic effect (Figure 6). The mutations in 7 out of 9 genes are in the intronic region and have no reported variant effect. At the same time, the mutations from KIT and TP53 are in the exonic region. Both are missense variants (Figure 6).

Discussion

Arsenic is recognized as a carcinogenic agent in the context of bladder cancer, lung cancer, and squamous cell carcinoma of the skin [14]. Nevertheless, its influence on breast cancer remains uncertain [8]. The present investigation proves that As_2O_3 has a more significant effect on non-tumoral breast cells when compared to double positive breast cancer cells. Also, the duration of exposure plays an essential part in stimulating malignant features.

The migratory and colony formation potential of MCF-10A cells subjected to As_2O_3 intoxication for a duration of 3 weeks resembles that of the control group. Conversely, MCF-10A_As_2O_3_6w demonstrated a noteworthy elevation in cell invasion, extracellular matrix degradation, and migratory activity. Similarly, another study where the exposure to As_2O_3 lasted for 24 weeks also reported arsenic to substantially increased the invasion capabilities of MCF-10A cells [15]. Our results show that in the MCF-10A_As_2O_3_6w cells, a maximum of five colonies were observed. However, these colonies were small and proved to be challenging to discern, indicating that the 6 weeks exposure to As_2O_3 did not fully stimulate the colony formation ability. Nonetheless, it is worth noting that As_2O_3 did demonstrate the capability to induce colony formation in soft agar after 25 passages, as reported in a previous study, but when these intoxicated cells were transplanted *in vivo*, they did not form tumors [16]. On the other hand, MCF-7 cells showed an increase in the invasion potential after 6 weeks of As_2O_3 intoxication, while having inhibited colony formation ability thus proving the dual role of As_2O_3 in this cell line.

In MCF-10A_As_2O_3_6w cells, there was a marked increase in the population of cells in the G2/M phase that was not observed at 3 weeks of intoxication. In MCF-7 cells exposed long-term to As_2O_3 there was no significant difference between experiments. The tendency of As_2O_3 to stimulate cell cycle progression in MCF-10A cells was seen also in the case of short-term intoxication. Earlier research by Liu Y. and colleagues [17] reported a significant elevation in the G2/M cell population for MCF-10A_As_2O_3 cells. Additionally, their study revealed that As_2O_3 leads to a time and dose-dependent increase in the expression levels of *Cell Division Cycle 6 (CDC6)* and *Cyclin D*. These markers provided evidence of cell cycle progression from G1 to S/G2 [17]. Conversely, it is noteworthy that arsenic was previously recognized as an agent that halts the cell cycle in the G2/M phase in MCF-7 cells [18-20]**.** However, in this context, it induces the cells to undergo apoptosis [19,21]. In our study, only in the case of short-term (24h) exposure to As_2O_3 in MCF-7_Ctr and MCF-7_As_2O_3_3w there was a reduction of G0 population, with a significant increase in G1 cells and a limited progression to G2/M. As follows, arsenic stimulates cell cycle progression (G2/M phase) to a higher degree in non-tumoral breast cells.

At the DNA level, As_2O_3 induces several mutations; some of which are similar in both types of cells: *KDR* (c.798+54G>A), *CSF1R* (c.*37AC>C, c.*35C>TC), *SMARCB1* (c.1119-41C>T), and *FLT3* (c.1310-3T>C). The *KDR* gene encodes a receptor for vascular endothelial growth factors. Some mutations in the *KDR* gene have previously been associated with a more favorable prognosis in breast cancer [22,23]. The elevated expression of the *CSF1R* gene in breast cancer has been associated with an unfavorable prognosis [24-26]. In the context of many cancers, *SMARCB1* is recognized as a tumor suppressor gene [27]. Nevertheless, the investigation of mutations within this gene concerning breast cancer is limited. A study identified *SMARCB1* mutations in 2 out of 122 breast cancer cases, with no apparent specific consequence in prognostic [28]. *FLT3* has a higher expression in breast cancer than in normal tissue, but it is associated with less aggressive forms of this malignancy. It stimulates immune cell infiltration at the tumor site [29].

In the case of MCF-10A_As_2O_3 cells, two genes exhibit specific mutations: *ERBB2* c.2307+46A>G and *ERBB4* c.421+58A>G. *ERBB2* (*HER2*) is a receptor for epidermal growth factor and it is known to be overexpressed in approximately 20-25% of breast cancer cases [30]. On the other hand, *ERBB4* functions to counteract the oncogenic activities of *ERBB2*. It has been linked to the resistance to tamoxifen treatment and is associated with the stimulation of cancer cell proliferation [31]. Mutations in these two genes might be precursors of malignant transformation considering that they are frequently mutated in the case of breast cancer.

MCF-7_As_2O_3_3w and MCF-7_As_2O_3_6w cells present specific mutations in *KIT* c.1594G>A and *TP53* c.215C>G. *KIT* is always present in normal breast epithelium. It is rarely expressed by breast cancer cells [32]. It has been suggested that the lack of *c-KIT* in breast cancer is associated with a less favorable prognosis and advanced stages [33]. Mutations in *KIT* most commonly occur in exon 11. However, an examination of mutations in the gastrointestinal tract revealed an exon 10 mutation (like the one induced by As_2O_3 in our study) present in a metastatic tumor, but absent in the primary site [34]. Breast cancer can involve mutations in the *TP53* gene, and these mutations are associated with an unfavorable prognosis [35]. The conserved region of *TP53*, encompassing exons 5 to 8, is the most common site targeted by mutations that result in missense mutations and the loss of tumor suppressor functions. Mutations occurring in exons 2 to 4, particularly those causing missense mutations, may lead to phenotypes that do not drive the malignant transformation of normal breast tissue [36]. In our study, the identified mutation was situated in exon 4 and it was categorized as benign.

As follows, in our study, mutations in MCF-10A_As_2O_3 cells are classified as either benign or of unknown clinical significance, likely because they are situated in intronic regions of the DNA. Conversely, mutations in *KIT* c.1594G>A and *TP53* c.215C>G, which are unique to MCF-7_As_2O_3 cells, are in exonic regions of the mRNA. Furthermore, arsenic elicits divergent mutations, with some potentially contributing to a more favorable prognosis in breast cancer, whereas others may result in a less favorable outlook for the disease.

Conclusions

In conclusion, our study reveals that As_2O_3 has a limited capacity to induce malignant transformation in normal cells, with a notable increase in invasive and migratory behavior, as well as cell cycle progression observed at the 6 weeks- mark of exposure. In estrogen/progesterone receptor positive breast cancer cells, As_2O_3 exhibits a dual role, both inhibitory and stimulatory. It leads to reduced colony formation ability at 6 weeks. It has no effect on cell migration, but it enhances cellular invasion. Interestingly, both normal and cancerous breast cells show signs of significant stress under long-term As_2O_3 treatment and the gain of several mutations that might have both cancer promoting and cancer inhibiting functions.

Acknowledgements

This study was funded by the Funding Agency—Ministry of Research and Innovation through the doctoral research project "Characterization of the molecular profile of hormone-dependent tumors" PCD—no. 1530/63/18 January 2018, by Funding Agency— Romanian Ministry of Research and Innovation, FPRD-UEFISCDI, within PNCDI, through the research project PN-III-P1-1.2-PCCDI2017-0737, ctr 35: "Genomic population mapping of radioactively and heavy metals contaminated areas in order to increase national security" (ARTEMIS), and by the Funding Agency—Ministry of Research and Innovation, CNCS-UEFISCDI, within PNCDI III through the research project PN-III-P4-ID-PCE-2016-0795, ctr 164/2017: "Addressing the complex exposome profile in hormone-dependent cancers of the breast and prostate and its influence on tumoral genome" (ACHILLE).

References

1. Sung H, Ferlay J, Siegel RL, Laversanne M, Soerjomataram I, Jemal A, et al. Global Cancer Statistics 2020: GLOBOCAN Estimates of Incidence and Mortality Worldwide for 36 Cancers in 185 Countries. CA Cancer J Clin. 2021;71:209-249.
2. Garcia-Closas M, Gunsoy NB, Chatterjee N. Combined associations of genetic and environmental risk factors: implications for prevention of breast cancer. J Natl Cancer Inst. 2014;106:dju305.
3. Bessonneau V, Rudel RA. Mapping the Human Exposome to Uncover the Causes of Breast Cancer. Int J Environ Res Public Health. 2019;17:189.
4. Chung JY, Yu SD, Hong YS. Environmental source of arsenic exposure. J Prev Med Public Health. 2014;47:253-257.
5. Vahter M, Concha G. Role of metabolism in arsenic toxicity. Pharmacol Toxicol. 2001;89:1-5.
6. Klein CB, Leszczynska J, Hickey C, Rossman TG. Further evidence against a direct genotoxic mode of action for arsenic-induced cancer. Toxicol Appl Pharmacol. 2007;222:289-297.
7. Schuhmacher-Wolz U, Dieter HH, Klein D, Schneider K. Oral exposure to inorganic arsenic: evaluation of its carcinogenic and non-carcinogenic effects. Crit Rev Toxicol. 2009;39:271-298.
8. Pullella K, Kotsopoulos J. Arsenic Exposure and Breast Cancer Risk: A Re-Evaluation of the Literature. Nutrients. 2020;12:3305.
9. Marciniak W, Derkacz R, Muszyńska M, Baszuk P, Gronwald J, Huzarski T, et al. Blood arsenic levels and the risk of familial breast cancer in Poland. Int J Cancer. 2020;146:2721-2727.
10. Marciniak W, Matoušek T, Domchek S, Paradiso A, Patruno M, Irmejs A, et al. Blood Arsenic Levels as a Marker of Breast Cancer Risk among BRCA1 Carriers. Cancers (Basel). 2021;13:3345.
11. Vu V, Navalkar N, Wei Y. Endocrine-disrupting metals in ambient air and female breast cancer incidence in US. Gynecol Endocrinol. 2019;35:1099-1102.
12. Budisan L, Gulei D, Jurj A, Braicu C, Zanoaga O, Cojocneanu R, et al. Inhibitory Effect of CAPE and Kaempferol in Colon Cancer Cell Lines-Possible Implications in New Therapeutic Strategies. Int J Mol Sci. 2019;20:1199.
13. Pop LA, Cojocneanu-Petric RM, Pileczki V, Morar-Bolba G, Irimie A, Lazar V, et al. Genetic alterations in sporadic triple negative breast cancer. Breast. 2018;38:30-38.
14. IARC Working Group on the Evaluation of Carcinogenic Risks to Humans. Arsenic, Metals, Fibres and Dusts. Lyon (FR): International Agency for Research on Cancer; 2012. (IARC Monographs on the Evaluation of Carcinogenic Risks to Humans, No. 100C.) ARSENIC AND ARSENIC COMPOUNDS. Available from: https://www.ncbi.nlm.nih.gov/books/NBK304380/
15. Xu Y, Tokar EJ, Waalkes MP. Arsenic-induced cancer cell phenotype in human breast epithelia is estrogen receptor-independent but involves aromatase activation. Arch Toxicol. 2014;88:263-274.
16. Soh MA, Garrett SH, Somji S, Dunlevy JR, Zhou XD, Sens MA, et al. Arsenic, cadmium and neuron specific enolase (ENO2, γ-enolase) expression in breast cancer. Cancer Cell Int. 2011;11:41.
17. Liu Y, Hock JM, Sullivan C, Fang G, Cox AJ, Davis KT, et al. Activation of the p38 MAPK/Akt/ERK1/2 signal pathways is required for the protein stabilization of CDC6 and cyclin D1 in low-dose arsenite-induced cell proliferation. J Cell Biochem. 2010;111:1546-1555.

18. Pruteanu LL, Braicu C, Módos D, Jurj MA, Raduly LZ, Zănoagă O, et al. Targeting Cell Death Mechanism Specifically in Triple Negative Breast Cancer Cell Lines. Int J Mol Sci. 2022;23:4784.
19. Zhao Y, Onda K, Sugiyama K, Yuan B, Tanaka S, Takagi N, et al. Antitumor effects of arsenic disulfide on the viability, migratory ability, apoptosis and autophagy of breast cancer cells. Oncol Rep. 2019;41:27-42.
20. Ling YH, Jiang JD, Holland JF, Perez-Soler R. Arsenic trioxide produces polymerization of microtubules and mitotic arrest before apoptosis in human tumor cell lines. Mol Pharmacol. 2002;62:529-538.
21. Laka K, Makgoo L, Mbita Z. Survivin Splice Variants in Arsenic Trioxide (As_2O_3)-Induced Deactivation of PI3K and MAPK Cell Signalling Pathways in MCF-7 Cells. Genes (Basel). 2019;10:41.
22. Dai X, Chen X, Hakizimana O, Mei Y. Genetic interactions between ANLN and KDR are prognostic for breast cancer survival. Oncol Rep. 2019;42:2255-2266.
23. Cui Y, Zhang P, Liang X, Xu J, Liu X, Wu Y, et al. Association of KDR mutation with better clinical outcomes in pan-cancer for immune checkpoint inhibitors. Am J Cancer Res. 2022;12:1766-1783.
24. Riaz N, Burugu S, Cheng AS, Leung SCY, Gao D, Nielsen TO. Prognostic Significance of CSF-1R Expression in Early Invasive Breast Cancer. Cancers (Basel). 2021;13:5769.
25. Aharinejad S, Salama M, Paulus P, Zins K, Berger A, Singer CF. Elevated CSF1 serum concentration predicts poor overall survival in women with early breast cancer. Endocr Relat Cancer. 2013;20:777-783.
26. Król M, Majchrzak K, Mucha J, Homa A, Bulkowska M, Jakubowska A, et al. CSF-1R as an inhibitor of apoptosis and promoter of proliferation, migration and invasion of canine mammary cancer cells. BMC Vet Res. 2013;9:65.
27. Kalimuthu SN, Chetty R. Gene of the month: SMARCB1. J Clin Pathol. 2016;69:484-489.
28. Mimori K, Inoue H, Shiraishi T, Ueo H, Mafune K, Tanaka Y, et al. A single-nucleotide polymorphism of SMARCB1 in human breast cancers. Genomics. 2002;80:254-258.
29. Chen R, Wang X, Fu J, Liang M, Xia T. High FLT3 expression indicates favorable prognosis and correlates with clinicopathological parameters and immune infiltration in breast cancer. Front Genet. 2022;13:956869.
30. Gaibar M, Beltrán L, Romero-Lorca A, Fernández-Santander A, Novillo A. Somatic Mutations in HER2 and Implications for Current Treatment Paradigms in HER2-Positive Breast Cancer. J Oncol. 2020;2020:6375956.
31. Brockhoff G. Target HER four in breast cancer? Oncotarget. 2019;10:3147-3150.
32. Simon R, Panussis S, Maurer R, Spichtin H, Glatz K, Tapia C, et al. KIT (CD117)-positive breast cancers are infrequent and lack KIT gene mutations. Clin Cancer Res. 2004;10:178-183.
33. Tsutsui S, Yasuda K, Suzuki K, Takeuchi H, Nishizaki T, Higashi H, et al. A loss of c-kit expression is associated with an advanced stage and poor prognosis in breast cancer. Br J Cancer. 2006;94:1874-1878.
34. Yim E, An HJ, Cho U, Kim Y, Kim SH, Choi YG, et al. Two different KIT mutations may lead to different responses to imatinib in metastatic gastrointestinal stromal tumor. Korean J Intern Med. 2018;33:432-434.
35. Li X, Chen X, Wen L, Wang Y, Chen B, Xue Y, et al. Impact of TP53 mutations in breast cancer: Clinicopathological features and prognosisImpact of TP53 mutations in breast CA. Thorac Cancer. 2020;11:1861-1868.
36. Hartmann A, Blaszyk H, McGovern RM, Schroeder JJ, Cunningham J, De Vries EM, et al. p53 gene mutations inside and outside of exons 5-8: the patterns differ in breast and other cancers. Oncogene. 1995;10:681-688.